ADCONIP 2014 Hiroshima

Optimization of Long Jump Landing Motion using Musculoskeletal System Simulation

Hiroki Yokota, Shigemichi Ohshima, Naoki Mizuno

Abstract—**Biomechanical modeling of the musculoskeletal system has become an important issue in human motion analysis. The scope of this paper is focused on the optimization of long jump landing using musculoskeletal system. In the long jump, athletes are affected by the dynamics of the sand pit that is different from a hard surface in the landing phase. Therefore, in order to obtain a good landing motion, it is necessary to analyze the dynamics of the sand and athlete simultaneously. The aim of this study is to obtain an optimal landing motion in the long jump by Multi-Objective Genetic Algorithm using a long jump model. This simulation model is composed of two elements, which are a musculoskeletal model and a landing pit model. The human body model is based on a multi body model containing eight rigid links and nineteen Hill-type muscles. The sand pit is modeled as particles assembly. Generally, it is very time-consuming to calculate an optimal motion and a particle calculation. Here, this paper proposed a floating sand pit model which is suited to the optimization of the landing motion. As examples, we performed two optimization problems which have different objective functions, and compared with each other.**

I. Introduction

Computational approaches using musculoskeletal models are used to study human movement and performance in lately [1]-[4]. Constructing a musculoskeletal model requires several different scientific disciplines, including biomechanics, anatomy, multi-body dynamics and computer science, among others. In particular, a forward dynamics simulation is needed to generate a dynamic human motion. The aim of this study is to create an optimal dynamic human motion in sports and exercise using the musculoskeletal system. From a sports performance point of view, movement optimization is of great interest to athletes, coaches, researchers and doctors. The scope of this paper is focused on the optimization of long jump landing motion.

The long jump has been a popular track and field event since the Ancient Greece Olympics. Athletes run up to a take-off board and without going past it jump as far as they can into a landing pit. The long jump is a dynamic event that comprises of the following four phases: approach run up, take-off, flight through the air, landing. Several studies have reported that approach velocity is highly related to performance [5], [6]. These studies have focused on approach and take-off phases in the long jump. However, in order to achieve the greatest jump distance, athletes should perform an optimal motion during flight and landing phases in addition to approach and take-off phases. To avoid injury in the landing phase, the landing area is filled sand that remain lose and give way easily during landing. Therefore, athletes are affected by the dynamics of the sand that is different from a hard surface. In order to obtain a good landing motion in the simulation, it is necessary to analyze the dynamics of the sand and athletes simultaneously. Little has been reported on the creating an optimal motion considering the effect of sand dynamics in the landing phase.

The purpose of this paper is to obtain the optimal landing motion in the long jump by modeling a human body and a sand pit, and simulate it coupling the human model and the sand pit model. The human body was modeled as a system of rigid bodies including muscle models to simulate the forward dynamics, and the sand pit was modeled as particles assembly using the discrete element method (DEM). Regarding the optimization of human motions using these models, DEM simulation are very time-consuming. Thus, this paper proposes the floating sand pit model which is suited to the optimization of the landing motion in the long jump. As examples of the long jump simulation using these models, we performed two optimization problems which have different objective functions. One of two optimization problem evaluated axial joint forces in addition to objective functions used by other problem. Two different optimal motions were presented and axial joint contact forces were compared with each other.

II. Musculoskeletal Model

A. Rigid body dynamics

The human body using in this study is modeled as a system of rigid bodies in the *xy*-plane. The model consists of eight rigid links and seven joints. The eight links represent the following eight body segments: the arm, the forearm, the hand, the upper body, the thigh, the shank, the foot and the toe.

The equation of motion for the entire body is the sum of the equations for each segment. A constraint on the positions of rigid bodies is represented by a constraint function $\mathbf{\Phi(q,t)}$. **This constraint is the function of the time and the position vector q. Position constraints can be divided into equality constraints (e.g., two bodies are connected by the joint). The constraint equation in this system is written as:**

$$\mathbf{\Phi}(\mathbf{q},t)=0 \tag{1}$$

H. Yokota is with Graduate School of Engineering, Department of Scientific and Engineering Simulation, Nagoya Institute of Technology, Gokiso-cho, Shouwa-ku, Nagoya, 466-8555, Japan (e-mail: h.yokota.848@stn.nitech.ac.jp).

S. Ohshima is with Department of Mechanical Engineering, Meijo University, 1-501, Shiogamaguchi, Tempaku-ku, Nagoya, 468-8502, Japan (e-mail: ohshi@meijo-u.ac.jp).

N. Mizuno is with Graduate School of Engineering, Department of Scientific and Engineering Simulation, Nagoya Institute of Technology, Gokiso-cho, Shouwa-ku, Nagoya, 466-8555, Japan (e-mail: nmizuno@nitech.ac.jp).

This equation is differentiated twice in order to introduce the accelerations:

$$\ddot{\mathbf{\Phi}} = \mathbf{J}\ddot{\mathbf{q}} + \frac{d\mathbf{J}}{dt}\dot{\mathbf{q}} + \frac{d^2\mathbf{\Phi}}{dt^2} = 0 \qquad (2)$$

where **J** is the constraint Jacobian matrix. The total force acting on the system is the sum of the external forces $\mathbf{Q}^A$ and the constraint forces $\mathbf{J}^T\Lambda$. Here, Λ is the coefficient vector whose components are called *Lagrange multipliers*. Combining the Newton-Euler equations with the constraint equations, we get the following differential algebraic equations

$$\begin{bmatrix} \mathbf{M} & \mathbf{J}^T \\ \mathbf{J} & 0 \end{bmatrix} \begin{bmatrix} \ddot{\mathbf{q}} \\ \Lambda \end{bmatrix} = \begin{bmatrix} \mathbf{Q}^A \\ -\gamma \end{bmatrix} \qquad (3)$$

which we can solve for the acceleration and the Lagrange multipliers. Here, **M** is the mass-matrix and γ is the additional term in the acceleration constraint that depends on the velocities. This equation was solved with a forth order Runge-Kutta numerical integration. However, it is well-known that this method has mild instabilities and drift problems, and consequently stabilization techniques have been proposed. In contrast to (2), Baumgarte proposed the modified function **N** that is defined to be

$$\mathbf{N} = \ddot{\mathbf{\Phi}} + 2\alpha\dot{\mathbf{\Phi}} + \beta^2\mathbf{\Phi} = 0 \qquad (4)$$

where α and β are constants to begin with [7]. The new constraint (4) is analytically equivalent to $\ddot{\mathbf{\Phi}}$=0. In this study, we utilized Baumgarte's technique to solve the stability problem for the numerical integration of constrained rigid body system.

The joints themselves exhibit resistance to movement because of the properties of cartilage and the shapes of the contacting articular surfaces. Conventionally, the joint passive resistance is modeled as an elastic element as spring and a viscous element like a rotary damper [8]. The viscous resistance effects constantly during a motion. The elastic resistance effects largely at the limit of range of motion of a joint. These two resistances can be expressed as follows:

$$\tau_p = \begin{cases} -c\dot{\theta} & \theta < \theta_{\lim} \\ k(\theta_{\lim} - \theta) - c\dot{\theta} & \theta \geq \theta_{\lim} \end{cases} \qquad (5)$$

where τ_p is the joint passive resistance, θ is the joint angle, θ_{lim} is the joint limit, k is the spring constant and c is the damping coefficient.

B. Muscle model

In this study, we utilized the muscle-like elastic actuators for a model based on the Hill-Stroeve muscle model [9], [10] which is a simplified version of the model of Winters and Stark [11]. For the purpose of modeling the muscle, algorithms refer to the force-length, and force velocity curves of the muscle. Figure 1 shows the musculoskeletal model of the entire body. This model consists of 19 muscle models and the above-mentioned rigid bodies. The muscle included in the model were the DLTc (anterior deltoid), BIC (biceps), BRA (brachialis), ECRl (extensor carpi radialis longus), DLTs (posterior deltoid), TRI (triceps), ANC (anconeus), FCR (flexor carpi radialis), IL (iliacus, psoas), RF (rectus femoris), VAS (vasti), TA (tibialis anterior), EXTDG (extensor digitorum longus, extensor halluces longus), GLM (gluteus maximus), HAM (medial hamstrings, biceps femoris long head), BFs (biceps femoris long head), GAS (gastrocnemius), SO (soleus) and FLXDG (flexor digitorum longus, flexor halluces longus).

Muscle force depends on the muscle length, velocity and activation; therefore, muscle force f is a function of muscle length l (= $l(t)$), muscle velocity $\dot{l}$ (= dl/dt) and activation a, such that:

$$f(a,l,\dot{l}) = a \cdot F_{lce}(l_{ce}) \cdot F_{vce}(\dot{l}_{ce}) \cdot F_{\max} \qquad (6)$$

where F_{lce}, F_{vce}, F_{max}, l_{ce} (= $l_{ce}(t)$) and $\dot{l}_{ce}$ (= dl_{ce}/dt) is the force-length relation, the force-velocity relation, the maximum isometric force, the length of contractile element and the contractile element velocity, respectively. The length and velocity of the muscle are given by:

$$l_i = l_{ri} - \sum_{j=1}^{7} r_{ij}(\theta_j - \theta_{rj}) \qquad (7)$$

$$\dot{l}_i = -\sum_{j=1}^{7} r_{ij}\dot{\theta}_j \qquad (8)$$

with l_r the rest length and r_{ij} the moment arm. The parameters r_{ij} specify the moment arms of muscle i (i = 1, ... ,19) with respect to joint j (j = 1, ... ,7). The rest positions of the joints (where passive torque is zero) is denoted θ_{rj}. The net joint torques exerted by the muscle are:

$$\tau_j = \sum_{i=1}^{19} r_{ij} f_i(a_i, l_i, \dot{l}_i) \qquad (9)$$

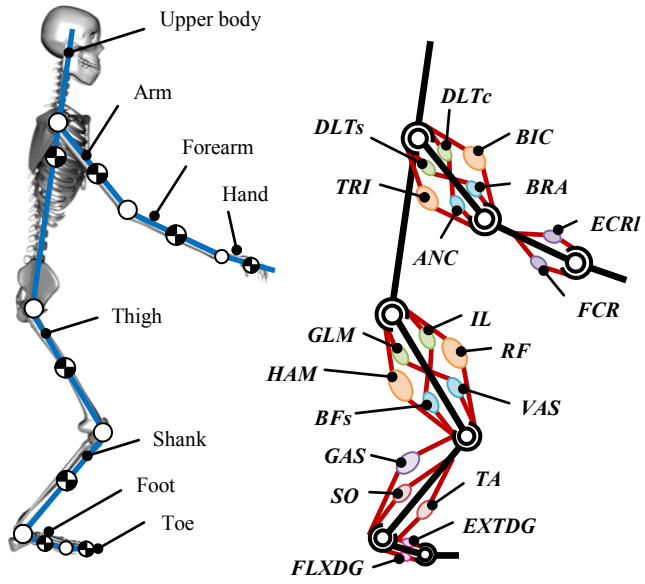

Figure 1. Musculoskeletal model of enter body including in muscle models.

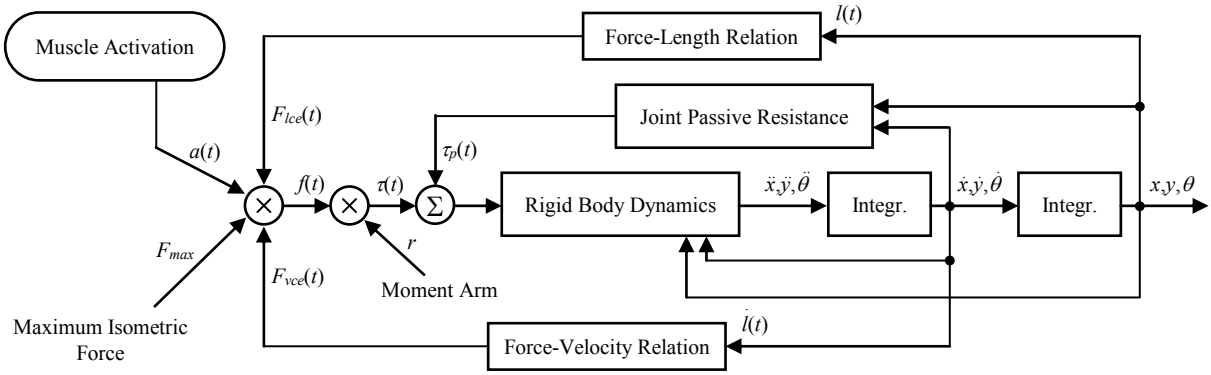

Figure 2. Schematic diagram of forward dynamics simulation using musculoskeletal system.

The moment arm values were determined by data provided by Meek [12] and Yamazaki [13]. The maximum isometric force was calculated from measured physiological cross-sectional area (PCSA) and a specific tension of 61 N/cm^2 for all muscles [14]-[16]. Figure 2 shows the schematic diagram of the musculoskeletal system. The muscle activation a is obtained by the optimization. The calculated muscle force is converted to the net joint torques, and then the joint torques and the joint passive resistances are inputted into the system of the rigid bodies. In short, the muscle activations generate the movement of each joint through several functions.

III. SAND PIT MODEL

A. Discrete Element Method

The sand pit is modeled as particles assembly using the discrete element method. DEM was introduced by Candall [17] for the analysis of rock mechanics problems and is being increasingly used to simulate the mechanical behavior of granular materials [18]. This method can describe the dynamics of individual particles. The model is composed of discrete particles that displace independent of one another, and interact only at contacts or interfaces between the particles. The particles collision model consists of several forces, including a spring force which forces the particle apart, and a dashpot force which causes damping. The motion of the particles is calculated by solving the Newton-Euler equations. In this study, the musculoskeletal model and this sand pit model were coupled together to solve the optimization problem of the long jump landing motion.

B. Floating sand pit model

Generally, DEM simulation is very time-consuming. The simulation time mainly depends on the critical time step and the particle number. Considering the long jump landing pit, particles are distributed over a large area. But in reality, to simulate this area using DEM would involve so many calculations that it is not considered practical. Therefore, in order effectively to perform the optimization regarding the landing motion, it is necessary to reduce calculation cost for DEM simulation. Here, this paper proposes the floating sand pit model which is suited to the optimization using DEM

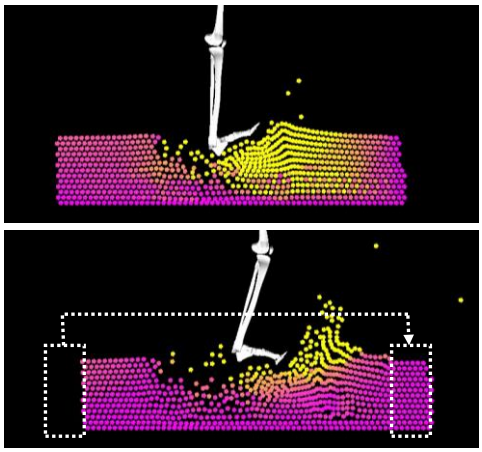

Figure 3. Coupled simulation using floating sand pit model.

simulation. The most attractive feature of this model is that it is not necessary to simulate the whole landing area, which reduces significantly the computational burden. Concerning the optimization of the landing motion, to calculate the specific area which is the neighborhood of the landing point is enough for it because analyzing the behavior of all sand particles is not important for motion optimization. This specific area is sequentially moved from backward place to forward place in accordance with the movements of the human model to prevent an increase of the number of particles. This means that the particle number is maintained constant during the landing simulation.

Figure 3 shows particles behavior by coupled simulation of the human model and the proposed floating sand pit model. The yellow particle represents a fast particle. This simulation started with the following some initial conditions; the human position was the origin, the horizontal velocity was 8.53 m/s, the vertical velocity was 3.52 m/s and muscle activations were set to zero over the simulation. It also confirmed that the coupled simulation considering the interaction between the human model and the sand pit model was achieved, and particles were moved from backward place to forward place.

IV. Optimization of Landing Motion

A. Multi-Objective Genetic Algorithm

Genetic Algorithms are search algorithms inspired by the mechanics of genetics and natural selection [19], [20]. These algorithms are a versatile tool, which can be applied to solve several complex optimization problems, because they are easy to implement to non-differentiable functions and discrete search. Regarding multi-objective optimization, several multi-objective genetic algorithms have been proposed in recent years [21]-[25]. In particular, Improving the Strength Pareto Evolutionary Algorithm (SPEA2) proposed by Zizler [26] has been reported to perform well in searching. SPEA2 is the improved algorithm of SPEA (Strength Pareto Evolutionary Algorithm) [27], which uses a regular population and an archive. The overall algorithm is as follows [26]:

Step 1: ***Initialization***: *Generate an initial population* $\boldsymbol{P}_0$ *and create the empty archive* $\boldsymbol{A}_0$.

Step 2: ***Fitness assignment***: *Calculate fitness values of individuals in* $\boldsymbol{P}_t$ *and* $\boldsymbol{A}_t$. *(t is number of iteration)*

Step 3: ***Environmental selection***: *Copy all nondoninated individuals in* $\boldsymbol{P}_t$ *and* $\boldsymbol{A}_t$ *to* $\boldsymbol{A}_{t+1}$. *If size of* $\boldsymbol{A}_{t+1}$ *exceeds archive size then reduce* $\boldsymbol{A}_{t+1}$ *by means of the truncation operator, otherwise if size of* $\boldsymbol{A}_{t+1}$ *is less than archive size then fill* $\boldsymbol{A}_{t+1}$ *with dominated individuals in* $\boldsymbol{P}_t$ *and* $\boldsymbol{A}_t$.

Step 4: ***Termination***: *If* $T \leq t$ *or another stopping criterion is satisfied then set nondoninated individuals to the set of decision vectors. Stop. (T is maximum number of generations).*

Step 5: ***Mating selection***: *Perform binary tournament selection with replacement on* $\boldsymbol{A}_{t+1}$ *in order to fill the mating pool.*

Step 6: ***Variation***: *Apply recombination and mutation operators to the mating pool and set* $\boldsymbol{A}_{t+1}$ *to the resulting population. Increment generation counter and go to Step 2.*

In contrast to SPEA, SPEA2 uses a fine-grained fitness assignment strategy which incorporates density information. In this paper, SPEA2 was used to search optimal design variables which are human parameters in the long jump landing. The design variables of the optimization problem are the muscle activations, which are plotted at 7 points per one muscle from 0 to 1.2 seconds at 0.2-second intervals. Thus, the number of design variables is 133. An interval between two points is interpolated using cubic spline interpolation. Individuals are represented as bit strings, where each bit corresponds to one decision variable. Each control point is represented by 10 bits; therefore, one individual has 1330 bit-length. The population size and end generation were set to 30 and 200. Recombination of two individuals is performed by two-point crossover. Point mutations are used where each bit is flipped with a probability of 0.02. In this section, we'll show two optimization results as examples, which are evaluated different objective functions.

B. Result of evaluating two objective functions (case: 1)

Two objective functions were considered in this optimization. The first objective function J_1 was set to maximize the jumping distance from a take-off board because the objective of the long jumping is to try and jump as far as possible. The second objective function J_2 was set to minimize the sum of squares of the muscle activations to solve the problem of multi-muscle and joint redundancy. It can be formulated as follows:

$$J_2 = \frac{1}{t_f}\int_0^{t_f}\sum_{i=1}^{19} a_{i_t}^2 dt \tag{10}$$

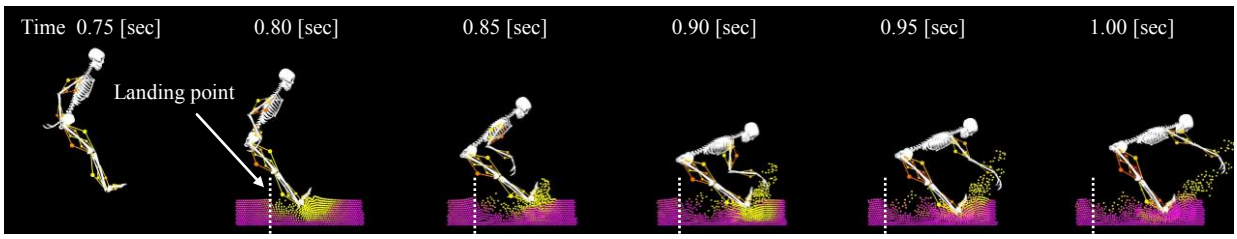

Figure 4. Optimal landing motion evaluated two objective functions at 200 generation (case: 1).

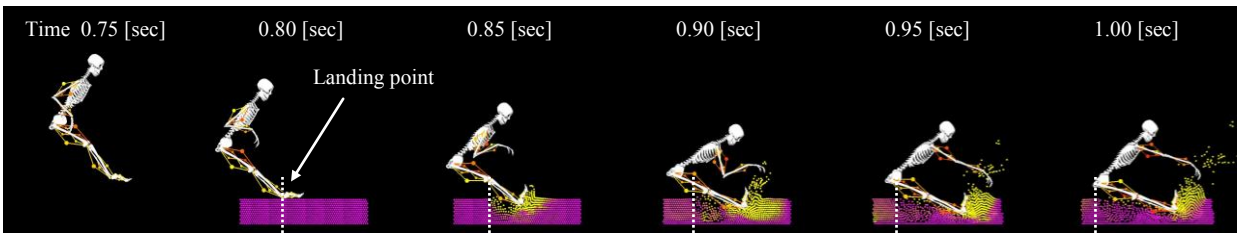

Figure 5. Optimal landing motion evaluated three objective functions at 200 generation (case: 2).

where t_f is the evaluation time. This simulation started with the same initial conditions as section III-B. Figure 4 shows the optimal landing motion at 200 generation in this simulation (case: 1). The vertical dotted line indicates the landing point in this jumping. In fig. 4, it was observed that the upper body was leaning forward in the landing phase. This trend can be seen particularly in weaker athletes and female athletes. After 0.76 seconds from simulation start, the human model landed in the sand pit.

C. Result of evaluating three objective functions (case: 2)

In addition to objective functions used by case: 1, one another objective function was considered in this optimization. The third objective function J_3 was set to minimize the maximal axial joint contact force to prevent the excessive load on joints in the landing phase. Figure 5 shows the optimal landing motion at 200 generation in this simulation (case: 2). It was observed that the hip was grounded at the end of the landing different from the result shown in fig. 4. Here, the human model landed in the sand pit after 0.80 seconds.

D. Discussion

Figure 6 shows typical muscle activations of the lower extremity in case: 1. In the landing phase, after 0.76 seconds from simulation start, typical muscles were activated slightly except the HAM. The VAS was activated and increased quickly, and the HAM was increased gradually thereafter. Thus, the human model was able to raise the upper body by activating the HAM constantly during the landing phase. Activating the VAS after the landing means that the human model kept the knee straight during landing phase. It seems that the knee joint was loaded the excessive load. On the other hand, other muscles were activated to produce coordinated contractions. Figure 7 shows typical muscle activations of the lower extremity in case: 2. In contrast to case: 1, the HAM was activated slightly during the landing phase. The VAS, RF and IL were activated rather than case: 1 at an earlier landing phase. It is suspected that the flight time was prolonged by activating these muscles to jump as far as possible. In the landing phase, the BFs and GAS activations were increased. It seems that an impact on the knee joint was relieved by bending the knee joint.

Figure 8 shows two different optimization results which are axial joint forces of the lower extremity over the long jump simulation. As shown in fig. 8a, axial joint forces had two major peaks during the landing phase, and had a higher peak

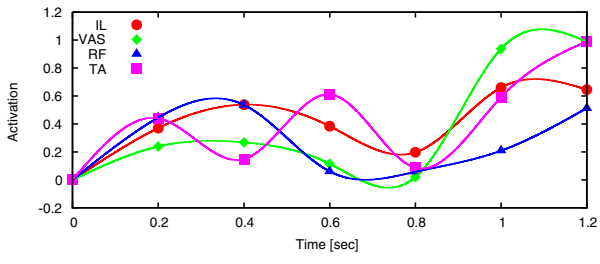

(a) Muscles in front of lower extremity.

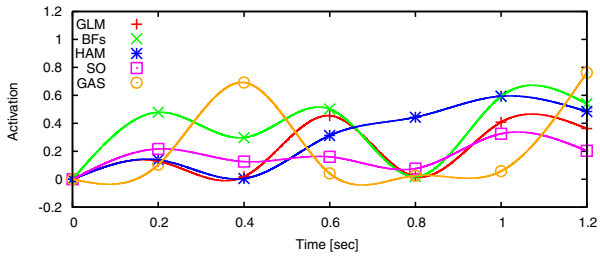

(b) Muscles in back of lower extremity.

Figure 6. Typical optimized muscle activation signals in lower extremity over long jump simulation in case: 1.

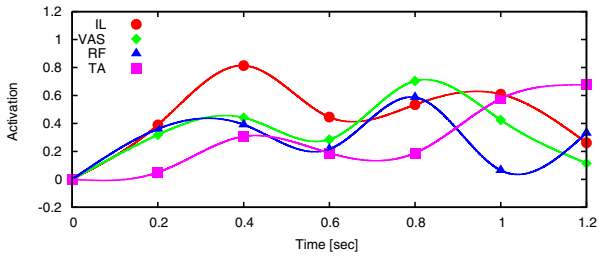

(a) Muscles in front of lower extremity.

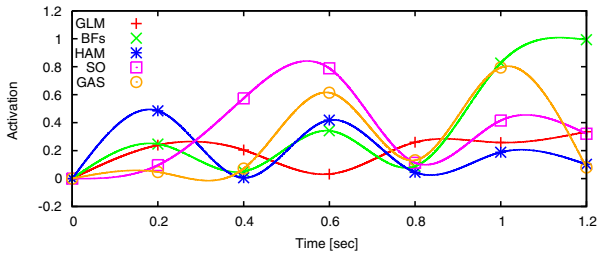

(b) Muscles in back of lower extremity.

Figure 7. Typical optimized muscle activation signals in lower extremity over long jump simulation in case: 2.

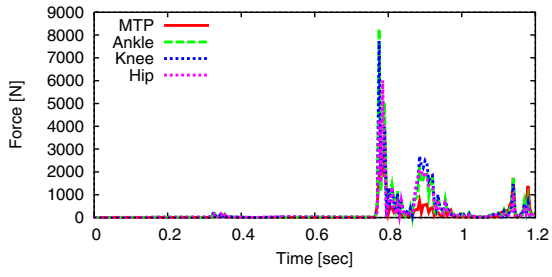

(a) Case: 1

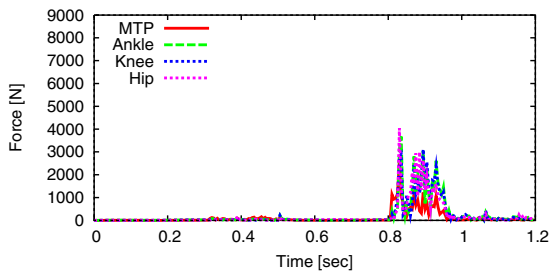

(b) Case: 2

Figure 8. Axial joint contact forces in lower extremity over long jump simulation .

value than case: 2 (fig. 8b). It confirmed that the cause of reducing axial joint contact forces is owing to slightly bending the knee on the landing time. To evaluate axial joint contact forces, we obtained the optimal landing motion to avoid injury.

V. Conclusion

In this work, we introduced the long jump model for the optimal landing motion. This simulation model comprises the human body model including 19 muscles, and the sand pit model which is suited to the optimization. As examples of the long jump simulation using this model, two different optimization problems regarding the long jump landing was solved with SPEA2. The results indicate that owing to slightly bending the knee on the landing, a competitor can prevent excess loads on lower extremity joints.

This simulation model can be applied to different situations in the long jump landing. As an example, we can perform the optimization that is assumed using the wet sand pit in rain weather by changing the parameters of the sand pit model.

References

[1] E. M. Arnold and S. L. Delp, "Fiber operating lengths of human lower limb muscles during walking," *Phil. Trans. Soc. B*, vol. 366, no. 1570, pp. 1530-1539, 2011.

[2] A. Erdemir, S. McLean, W. Herzog, and A. J. van den Bogert, "Model-based estimation of muscle forces exerted during movements," Clinical Biomechanics, vol. 22, no. 2, pp. 131-154, 2007.

[3] A. Carvalho and A. Suleman, "Multibody simulation of the musculoskeletal system of the human hand," *Multibody System Dynamics*, vol. 29, pp. 271-288, 2013.

[4] H. Böhm, C. Krämer, and V. Senner, "Optimization of the handbike's drive concept — Mathematical approach," *Springer, The Engineering of Sport 6*, vol. 2, pp. 121-125, 2006.

[5] L. A. Bridgett and N. P. Linthome, "Changes in long jump take-off technique with increasing run-up speed," *Journal of sports science*, vol. 24, no. 8, pp. 889-897, 2006.

[6] N. A. Moura, T. F. Paula Moura, and J. P. Borin, "Approach speed and performance in the horizontal jump : What do Brazilian athletes do?," *New studies in athletics*, vol. 20, no. 3, pp. 43-48, 2005.

[7] J. Baumgarte, "Stabilization of constraints and integrals of motion in dynamical systems," *Computer methods in applied mechanics and engineering*, vol. 1, pp. 1-16, 1972.

[8] J. F. Lamb, C. G. Ingram, I. A. Johnston, and R. M. Pitman, "Essentials of physiology," *Blackwell Scientific Publications*, 1991.

[9] S. Stroeve, "Impedance characteristics of a neuromusculoskeletal model of the human arm I. Posture control," *Journal of Biological Cybernetics*, vol. 81, pp. 475-494, 1999.

[10] A. Hill, "The heat of shortening and the dynamic constants of muscle," In *Proceeding of the Royal Society of London*, vol. 126, pp. 136-195, 1938.

[11] J. M. Winters and L. Stark, "Analysis of fundamental human movement patterns through the use of in-depth antagonistic muscle models," *IEEE Trans Biomed Eng*, vol. 32, pp. 826-839, 1985.

[12] S. G. Meek, J. E. Wood, and S. G. Jacobsen, "Model-based, multi-muscle EMG control of upper-extremity prostheses," *Multiple Muscle Systems: Biomechanics and Movement Organization*, pp. 360-376, 1990.

[13] N. Yamazaki, "Analysis model and simulation of the biped locomotion," *Biomechanisms*, vol. 3, pp. 261-269, 1975, (in Japanese).

[14] K. R. S. Holzbaur, W. M. Murray, G. E. Gold, and S. L. Delp, "Upper limb muscle volumes in adult subjects," *Journal of Biomechanics*, vol. 40, pp. 742-749, 2007.

[15] E. M. Arnold, S. R. Ward, R. L. Lieber, and S. L. Delp, "A model of the lower limb for analysis of human movement," *Annals of Biomedical Engineering*, vol. 38, no. 2, pp. 269-279, 2010.

[16] S. R. Ward, C. M. Eng, L. H. Smallwood, and R. L. Lieber, "Are current measurements of lower extremity muscle architecture accurate?," *Clin. Orthop. Relat. Res.*, vol. 467, pp. 1074-1082, 2009.

[17] P. A. Candall, "A computer model for simulating progressive large scale movements in blocky rock systems," In *Proceedings of the Symposium of the International Society of Rock Mechanics*, vol. 1, paper II-8, 1971.

[18] P. A. Candall and O. D. L. Strack, "A discrete numerical model for granular assemblies," *Geotechnique*, vol. 29, no. 1, pp. 47-65, 1979.

[19] J. H. Holland, "Adaptation in natural and artificial systems," University of Michigan Press, 1975.

[20] D. E. Goldberg, "Genetic algorithms in search, optimization, and machine learning," Addison-Wesley, 1989.

[21] J. D. Schaffer, "Multiple objective optimization with vector evaluated genetic algorithms," In *Genetic Algorithms and Their Applications: Proceedings of 1st International Conference on Genetic Algorithms*, pp. 93-100, 1985.

[22] C. M. Fonseca and P. J. Fleming, "Genetic algorithms for multiobjective optimization: formulation, discussion and generalization," In *Proceedings of the 5th International Conference on Genetic Algorithms*, pp. 416-423, 1993.

[23] N. Srinivas and Kalyanmoy Deb, "Multiobjective optimization using nondominated sorting in genetic algorithms," *Evolutionary Computation*, vol. 2, no. 3, pp. 221-248, 1994.

[24] J. Horn, N. Nafpliotis, and D. E. Goldberg, "A niched pareto genetic algorithm for multiobjective optimization," In *Proceedings of the 1st IEEE Conference on Evolutionary Computation, IEEE World Congress on Computational Intelligence*, vol. 1, pp.82-87, 1994.

[25] E. Zizler and L.Thiele, "Multiobjective evolutionary algorithms: a comparative case study and the strength pareto approach," *IEEE Transactions on Evolutionary Computation*, vol. 3, no. 4, pp. 257-271, 1999.

[26] E. Zizler, M. Laumanns, and L. Thiele, "Spea2: Improving the strength Pareto evolutionary algorithm," *Evolutionary Methods for Design, Optimization and Control with Applications to Industrial Problems*, pp. 95-100, 2001.

[27] E. Zitzler and L. Thiele, "Multiobjective evolutionary algorithms: a comparative case study and the strength pareto approach," *IEEE Transactions on Evolutionary Computation*, vol. 3, no. 4, pp. 257-271, 1999.